

---

# The Isomers of Ionized Ethane

---

CHARLES E. HUDSON\* and DAVID J. MCADOO

*Marine Biomedical Institute, The University of Texas Medical Branch, Galveston, Texas 77555*

C. S. GIAM

*Department of Marine Sciences, Texas A & M University at Galveston, Galveston, Texas 77551*

*Received 24 May 1995; accepted 15 November 1995*

---

## ABSTRACT

The previously reported  $^2A_g$ ,  $^2A_{1g}$ , and  $^2B_g$  states of ionized ethane are characterized at several levels of theory. The diborane-like  $^2A_g$  state, which gives rise to the observed ESR spectrum, is predicted by SCF and CCD calculations not to exist in a separate minimum from the  $^2A_{1g}$  state formed by ionization of the C—C bond. However, as reported by Lunell and Huang, second-order Moller–Plesset theory places the  $^2A_g$  lowest, provided polarization functions are included on carbon. QCISD theory predicts that both  $A$  states correspond to potential energy minima, but places the long-bond  $^2A_{1g}$  state lower, at least with moderately large basis sets. F orbitals on carbon stabilize the diborane structure more than the long-bond one. When a potential energy surface is generated for a series of fixed C—C bond lengths by optimizing all variables except for the C—C bond length with MP2 theory and calculating the energy with QCISD(T), the  $^2A_g$  state is predicted to be the lowest energy state with the  $^2A_{1g}$  state 1.83 kJ/mol above it. The two  $A$  states are predicted to be separated by a barrier 2.79 kJ/mol above the lower state. This barrier is above the zero-point energy in the C—C stretch for the lower state but below the ZPE for this stretch in the upper state, which is therefore predicted not to exist as a stable species. A single quantum of vibrational excitation in the low frequency C—C stretch is predicted to yield an ion with a poorly defined C—C bond length. The highest levels of theory employed give poor agreement with the experimental hyperfine coupling constants. The discrepancy could either be due to neglect of vibrational effects, to poor inherent accuracy of the calculation, as one author has concluded, or to compression of the ion by the matrix as suggested by another. The  $^2B_g$  state is found to be higher in energy than the  $A$  states at all theoretical levels and is predicted to have a large (160.2–177.4 G) hyperfine coupling from four hydrogens. The transition state for simultaneous exchange of two hydrogen atoms between the carbons by a diborane structure is predicted to lie above the lowest energy fragmentation threshold, in agreement with experiment. © 1996 by John Wiley & Sons, Inc.

\*Author to whom all correspondence should be addressed.

## Introduction

For several years, a paradox existed in the chemistry of ionized ethane. Table I<sup>1</sup> shows that, in neutral ethane, the C—C bond is the weakest in the molecule:  $\Delta H_f(2\text{CH}_3) = 291.6$  kJ/mol,  $\Delta H_f(\text{C}_2\text{H}_5 + \text{H}) = 336$  kJ/mol. However, in the ethane cation radical the weakest bond is one of the C—H bonds:  $[\Delta H_f(\text{CH}_3^+ + \text{CH}_3) = 1239.1$  kJ/mol,  $\Delta H_f(\text{C}_2\text{H}_5^+ + \text{H}) = 1120$  kJ/mol. This would be easy to understand if the ionization took place from an orbital primarily devoted to C—H bonding. However, a fairly high level calculation<sup>2</sup> predicted that the lowest energy state of the ethane cation results from removal of an electron from the C—C bond. This should weaken the C—C bond in the ion more than the C—H bond. Moreover, the ESR spectrum of the ion in a matrix of low reactivity<sup>3</sup> is completely inconsistent with a C—C ionized state. The discrepancy is so glaring that one investigator<sup>4</sup> suggested that the matrix was distorting the ion in the ESR experiment. These difficulties were resolved in 1989 by Lunell and Huang.<sup>5</sup> They showed that the  $^2A_g$  state arising by ionization from the C—H bonding  $e_g$  HOMO (highest occupied molecular orbital) is predicted to be more stable than the C—C ionized  $^2A_{1g}$  state, provided that polarization functions were used on both types of atoms in the ion and that electron correlation was taken into account using second-order Moller–Plesset (MP2) theory. This state was predicted to have a geometry intermediate between those of neutral ethane and diborane.

Thus, when our work began, the study with the more extensive treatment of correlation<sup>2</sup> predicted that the ground state of  $\text{C}_2\text{H}_6^+$  should have a long C—C bond and small hyperfine splittings from the hydrogens. In contrast, the studies with the larger basis set<sup>5</sup> predicted that  $\text{C}_2\text{H}_6^+$  should have a

nearly normal C—C bond, and two long C—H bonds with acute HCC bond angles and two large hyperfine splittings from these hydrogens. While the latter is certainly required by the ESR experiment, this does not separate the effects of the matrix from the intrinsic properties of the ion.

Richartz et al.<sup>2</sup> found that there are three states which might contribute significantly to the photoelectron spectrum of ethane. The HOMO of ethane is a doubly degenerate ( $e_g$ ) pair of orbitals which are primarily devoted to C—H bonding and whose individual symmetry is  $C_{2h}$ . They are designated  $a_g$  for the MO that is symmetrical with respect to the plane of symmetry that the  $C_{2h}$  point group has and  $b_g$  for the complementary antisymmetrical MO. The third orbital of low ionization energy was calculated to be a totally symmetric  $a_{1g}$  orbital having the full  $D_{3d}$  symmetry of the neutral and devoted to C—C  $\sigma$  bonding. Removal of an electron from this orbital results in an ion with a long C—C bond.<sup>2,4</sup> The states are named with capital letters and have the same symmetry as the singly occupied orbitals they contain. The  $e_g$  orbitals have an antibonding interaction of  $\pi$  character between the carbons.<sup>6</sup> Removal of an electron from  $b_g$  component of the degenerate HOMO results, after Jahn–Teller distortion, in an ion with four elongated bonds to the hydrogens off the symmetry plane and a C—C bond with a length intermediate between typical single and double bonds similar to that in ferrocene. Richartz et al. referred to this  $^2B_g$  state as an antidiborane structure.<sup>2</sup> In the  $C_{2h}$  point group, the  $^2A_g$  and  $^2A_{1g}$  states have the same symmetry, and can mix. Removal of an electron from the  $a_g$  component of the HOMO results in the structure found by Lunell and Huang discussed above. The C—C bond length of this state depends on the degree of admixture with the  $^2A_{1g}$  state, which in turn depends on the manner in which electron correlation is treated. With unrestricted Hartree–Fock (UHF) theory the  $^2A_g$  state does not exist as a separate minimum.<sup>4,6</sup> Another study<sup>7</sup> using quadratic configuration interaction with single and double excitations (QCISD) methods found only the long-bond state, although it is not clear how hard they looked for the diborane form. Thus, there is a disagreement in the literature as to the identity of the ground state of ionized ethane, which we sought to resolve with higher level calculations. We also wanted to try various theoretical methods to estimate the barrier (if any) between the symmetric states and to characterize the  $^2B_g$  state.

**TABLE I.**  
Heats of Formation (kJ/mol)<sup>a</sup>.

Formula	H	CH <sub>3</sub>	C <sub>2</sub> H <sub>5</sub> ( $D_{C-H}$ )	— ( $D_{C-C}$ )
$\Delta H_f$ (neutral)	218.0	145.8	118.0	44.4
$\Delta H_f$ (positive ion)	1528.0	1093.3	902.0	— 119

<sup>a</sup>Based on values in Ref. 1.

## Results and Discussion

Table II gives our results for the energies of the three states and Table III presents the corresponding structural parameters. Note that the order of the symmetric states is reversed depending upon whether correlation is treated with MP2 or QCISD methods. Addition of a second set of  $d$  orbitals on the carbons and a second set of  $p$  orbitals on hydrogen stabilizes the long-bond form slightly more than the diborane ( $^2A_g$ ) form. Adding  $f$  orbitals to the carbons in MP2 theory lowers the energies of both the  $^2A_g$  and  $^2B_g$  states substantially with respect to the  $^2A_{1g}$  state. MP2 methods

predict a C—C bond length for the  $^2A_g$  state similar to that of the neutral, while QCISD theory predicts a bond 0.13–0.17 Å longer. Part of this difference may be due to the fact that our MP2 calculations treat all electrons, while the QCI calculations are frozen core. In our experience, freezing the core always increases the bond length, typically by about  $2 \times 10^{-3}$  Å for bonds between first row elements and about half as much for bonds between first row elements and hydrogen. However  $C_2H_6^+$  is not a typical case. A run optimizing the diborane form with MP2 = frozen core in the 6-311 + G\*\* basis set has a C—C bond  $6.0 \times 10^{-3}$  Å longer than the optimization with MP2 = full in the same basis set.

**TABLE II.**  
Energies of Ionized Ethane Species.

Species	$^2A_g$	$^2A_{1g}$	TS	$^2B_g$
A//A	-79.184768	-79.182174	-79.181876	-79.178219
ZPVE, <sup>a</sup> kJ/mol	182.73	183.25	182.46	186.20
$\Delta E$ , <sup>b,c</sup> kJ/mol	0	4.70	7.32	20.56
F//A	-79.191650	-79.191565	-79.191180	-79.181925
$\Delta E(2df)$	-0.035466	-0.034330	-0.034385	-0.037542
$\Delta E(QCI)$	-0.002263	-0.002426	-0.002629	-0.001536
$\Delta E(GI)$ <sup>d</sup>	0	3.30	2.84	25.56
G//A	-79.192628	-79.192368	-79.192177	-79.183289
$\Delta E$ , <sup>b,c</sup> kJ/mol	0	1.20	0.91	27.99
B//B	-79.208099	-79.206810	-79.206309	-79.202128
$\Delta E$ , <sup>b,c</sup> kJ/mol	0	3.90	4.43	19.15
H//B	-79.211359	-79.212515	-79.211830	-79.202245
$\Delta E$ , <sup>b,c</sup> kJ/mol	0	-2.52	-1.53	27.39
I//B	-79.212389	-79.213324	-79.212918	-79.203644
$\Delta E$ , <sup>b,c</sup> kJ/mol	0	-1.93	-1.66	26.38
C//C	-79.231005	-79.227955	-79.227666	-79.225833
$\Delta E$ , <sup>b,c</sup> kJ/mol	0	8.53	8.49	17.05
J//C	-79.236585	-79.236678	-79.236495	-79.227826
$\Delta E$ , <sup>b,c</sup> kJ/mol	0	0.28	-0.03	26.47
D//D	-79.185932	-79.186581	-79.185928	-79.172322
$\Delta E$ , <sup>b,e</sup> kJ/mol	0	-1.44	0.01	35.73
COMPOSITE <sup>f</sup>	-79.237390	-79.236694	-79.236329	
$\Delta E$ , <sup>b,e</sup> kJ/mol	0	1.83	2.79	
E//E	-79.218161	-79.218606		
$\Delta E$ , <sup>b,e</sup> kJ/mol	0	-1.17		
K//E	-79.229157	-79.228068		
$\Delta E$ , <sup>b,e</sup>	0	2.86		

Methods: A = MP2/6-311+G\*\*, B = MP2/6-311+G(2d,2p), C = MP2/6-311+G(2df,2p), D = QCISD/6-311+G\*\*, E = QCISD/6-311+G(2df,p), F = MP4(SDTQ)/6-311+G\*\*, G = PMP4/6-311+G\*\*, H = MP4(SDTQ)/6-311+G(2d,2p), I = PMP4/6-311+G(2d,2p), J = QCISD(T)/6-311+G(2df,2p), K = QCISD(T)/6-311+G(2df,p).

<sup>a</sup>Calculated numerically using method A.

<sup>b</sup>Relative to the  $^2A_g$  state.

<sup>c</sup>Includes ZPVE.

<sup>d</sup>The G1 energy is C//A +  $\Delta E(2df)$  +  $\Delta E(QCI)$  + ZPVE.

<sup>e</sup>Electronic energy only.

<sup>f</sup>See text.

**TABLE III.**  
**Optimized Parameters of Ethane Ions.**

Species		${}^2A_g$	${}^2A_{1g}$	TS	${}^2B_g$
RCC	A	1.5764	1.9064	1.8529	1.4359
	B	1.5828	1.9209	1.8368	1.4308
	C	1.5558	1.9078	1.8523	1.4272
	D	1.7470	1.9171	1.7820	1.4385
	E	1.6883	1.9241		
	F	1.6546	1.9198	1.8657	
RCH1 <sup>a</sup>	A	1.1412	1.0871	1.0942	1.0859
	B	1.1339	1.0798	1.0904	1.0791
	C	1.1406	1.0809	1.0884	1.0799
	D	1.1108	1.0899	1.1062	1.0879
	E	1.1185	1.0876		
	F	1.1207	1.0808	1.0811	
RCH2 <sup>b</sup>	A	1.0863	1.0871	1.0856	1.1396
	B	1.0789	1.0798	1.0781	1.1344
	C	1.0804	1.0809	1.0794	1.1346
	D	1.0877	1.0899	1.0878	1.1431
	E	1.0857	1.0876		
	F	1.0792	1.0808	1.0811	
H1CC <sup>a</sup>	A	82.21	98.38	88.80	118.54
	B	82.42	98.03	86.55	118.60
	C	82.87	98.09	88.49	118.74
	D	83.13	98.37	84.26	118.56
	E	82.35	98.16		
	F	80.89	97.97	98.52	
H2CC <sup>b</sup>	A	115.47	98.38	104.20	112.25
	B	115.22	98.03	105.53	112.19
	C	115.95	98.09	104.05	112.26
	D	109.71	98.37	108.27	112.22
	E	111.83	98.16		
	F	113.29	97.97	98.52	
H1CCH2 <sup>c</sup>	A	70.04	60.	61.62	45.81
	B	69.69	60.	62.34	45.91
	C	70.55	60.	61.64	45.80
	D	64.81	60.	63.82	46.02
	E	66.45	60.		
	F	68.01	60.	60.00	

A = MP2/6-311+G\*\*, B = MP2/6-311+G(2d,2p), C = MP2/6-311+G(2df,2p), D = QCISD/6-311+G\*\*, E = QCISD/6-311+G(2df,p), F = COMPOSITE (see text).

<sup>a</sup>Bond length (angle) for the two hydrogens in the plane of symmetry.

<sup>b</sup>Bond length (angle) to the other four equivalent hydrogens.

<sup>c</sup>Dihedral angle between the plane of symmetry and the H2CC plane.

It would be desirable to optimize the structure of  $C_2H_6^+$  in the 6-311+G(2df,2p) basis set using the QCISD correlation treatment. However, that was not feasible because of the space and time requirements of the task and the limits of the

computational facilities. Consequently, we fixed the C—C bond length at several different values and optimized the other parameters with MP2 theory. We then evaluated the energies at these optimized geometries using QCISD(T). The resulting data are presented in Figure 1. The data points near the energy extrema were fitted to parabolas. The coordinates of the vertices of these parabolas are presented in the tables on the line labeled "COMPOSITE." A very similar structure was arrived at by Eriksson and Lunell using MP4 optimization in a smaller basis set.<sup>8</sup> However, a density-functional theory study of this ion predicted a much shorter C—C bond than is found at any other level of theory.<sup>9</sup> Figure 1 and the derived numbers in Table II predict that the minimum of the  ${}^2A_{1g}$  state lies 1.83 kJ/mol above that of the  ${}^2A_g$  state with a barrier separating them 2.79 kJ/mol above the latter state. Thus, the  ${}^2A_g$  state is probably the ground state of  $C_2H_6^+$ . Figure 2 presents a view of the ion with the structure optimized in this way. The height of this barrier is given at several levels of theory in Table II. At our highest level of theory we find that the total variation in electronic energy over C—C bond lengths is 1.5558–1.95 Å is less than 3 kJ/mol. Because of the small difference in energy between the symmetric states and the low barrier between them, the issue of whether the C—H or C—H bonds is weaker in the ion depends more on the nature of the products and the transition states leading to

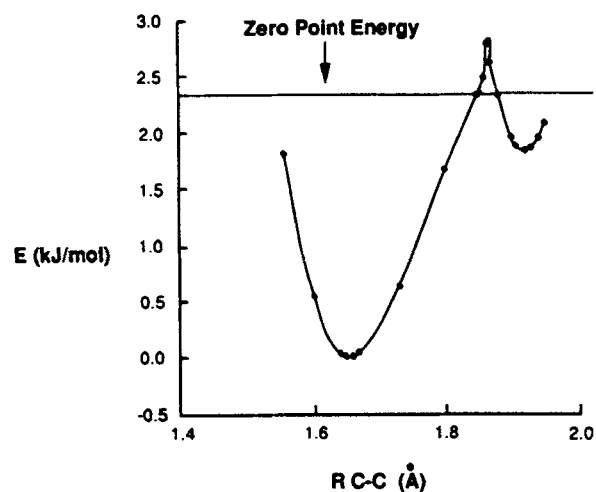


**FIGURE 1.** Energy versus C—C bond length in the ethane cation. Structures were optimized at the indicated C—C bond lengths using MP2 theory and the energies of the optimized structures were then determined using QCISD(T) theory (see text).

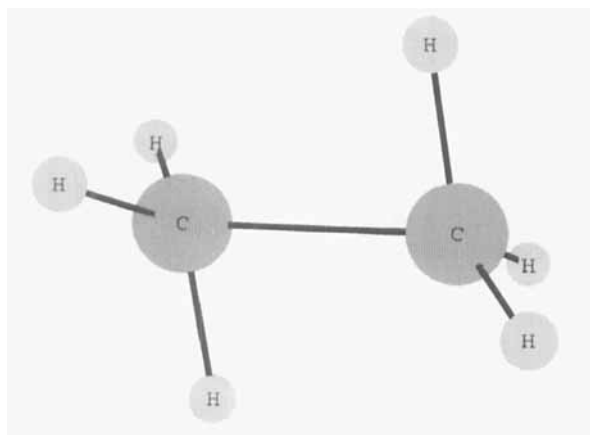


**FIGURE 2.** View of the ground state of ionized ethane as optimized by the composite method (see text) in the 6-311 + G(2df,2p) basis set.

them than upon the site of lowest energy ionization.

Vibrational frequencies were calculated at the MP2/6-311 + G\*\* stationary points (Table IV). Another study of the  $^2A_g$  state has appeared while this one was in preparation.<sup>8</sup> The vibrational frequencies calculated by these authors using MP2/6-31G\*\* methodology generally differ from ours by 65  $\text{cm}^{-1}$  or less. Our frequencies are 25  $\text{cm}^{-1}$  lower than theirs on average, while the RMS difference is 42  $\text{cm}^{-1}$ . The lowest energy mode for all three states is predicted by our method to be the torsion about the C—C bond. The C—C stretching vibration is assigned to the 531  $\text{cm}^{-1}$  vibration in the  $^2A_g$  state and to the 509  $\text{cm}^{-1}$  vibration in the  $^2A_{1g}$  state on the basis of the symmetry, large reduced mass, and displacements (not given for brevity). These frequencies both correspond to zero-point vibrational energies (ZPVEs) of more than 3 kJ/mol. This opened the possibility that the ion might be fluxional, having no well-defined C—C bond length between about 1.5 and 2.0 Å. The parabolas used to analyze Figure 1 also yield force constants. Combined with the reduced masses calculated for the C—C stretching vibrations in Table IV we derive  $390 \pm 3 \text{ cm}^{-1}$  for this mode in the  $^2A_g$  state and  $572 \pm 3 \text{ cm}^{-1}$  in the  $^2A_{1g}$  state. These correspond to ZPVEs of  $2.33 \pm 0.02 \text{ kJ/mol}$  and  $3.42 \pm 0.01 \text{ kJ/mol}$ , respectively. These estimates of the vibrational frequencies and ZPVEs should be better than the MP2/6-311 + G\*\* results discussed previously because they are derived from a larger basis set and a more elaborate treatment of correlation. Hence, our calculations predict that for the  $^2A_g$  state the ZPVE in the C—C stretch is less than the

**TABLE IV.**  
Vibrational Frequencies,<sup>a</sup> Symmetries,<sup>b</sup> and  
Reduced Masses<sup>c</sup> of Ionized Ethane Species.

Species	$^2A_g$	$^2A_{1g}$	TS	$^2B_g$
297 $A_u$	251 $A_{1u}$	302i $A_g$	301 $A_u$	
(1.012)	(1.008)	(1.684)	(1.048)	
531 $A_g$	354 $E_g$	238 $A_u$	471 $B_g$	
(5.383)	(1.144)	(1.008)	(1.344)	
567 $B_u$	354 $E_g$	610 $B_g$	669 $A_u$	
(1.047)	(1.144)	(1.129)	(1.040)	
859 $A_u$	509 $A_{1g}$	635 $A_g$	763 $B_u$	
(1.036)	(4.971)	(2.347)	(1.066)	
952 $B_g$	695 $E_u$	701 $B_u$	882 $B_g$	
(1.059)	(1.014)	(1.018)	(1.179)	
1078 $A_g$	695 $E_u$	722 $A_u$	1115 $A_g$	
(1.343)	(1.014)	(1.013)	(1.514)	
1186 $A_g$	1255 $A_{2u}$	1242 $B_u$	1166 $A_g$	
(1.075)	(1.229)	(1.226)	(1.273)	
1192 $A_u$	1324 $A_{1g}$	1305 $A_g$	1252 $A_u$	
(1.070)	(1.139)	(1.106)	(1.077)	
1245 $B_u$	1440 $E_u$	1388 $A_u$	1298 $A_g$	
(1.199)	(1.094)	(1.096)	(1.730)	
1253 $B_g$	1440 $E_u$	1414 $B_g$	1411 $B_u$	
(1.309)	(1.094)	(1.131)	(1.140)	
1489 $B_u$	1455 $E_g$	1464 $B_u$	1517 $A_g$	
(1.080)	(1.109)	(1.091)	(1.348)	
1524 $A_g$	1455 $E_g$	1475 $A_g$	1991 $B_u$	
(1.060)	(1.109)	(1.087)	(1.013)	
2673 $B_u$	3109 $A_{2u}$	3081 $B_u$	2583 $B_g$	
(1.070)	(1.012)	(1.020)	(1.035)	
2717 $A_g$	3118 $A_{1g}$	3083 $A_g$	2624 $A_u$	
(1.069)	(1.011)	(1.019)	(1.062)	
3196 $A_g$	3287 $E_g$	3248 $A_g$	2844 $A_g$	
(1.068)	(1.115)	(1.103)	(1.093)	
3197 $B_u$	3287 $E_g$	3269 $B_u$	3234 $B_u$	
(1.057)	(1.115)	(1.111)	(1.069)	
3294 $B_g$	3306 $E_u$	3309 $B_g$	3246 $A_g$	
(1.122)	(1.119)	(1.119)	(1.101)	
3301 $A_u$	3306 $E_u$	3318 $A_u$	3761 $B_u$	
(1.114)	(1.119)	(1.118)	(1.167)	

<sup>a</sup>Per  $\text{cm}^{-1}$ .

<sup>b</sup>Letters represent symmetry designation.

<sup>c</sup>In parentheses.

barrier between the states. The  $^2A_{1g}$  minimum is only 0.96 kJ/mol below the top of the barrier. The ZPVE in the C—C stretch makes the energy of the  $^2A_{1g}$  state 2.46 kJ/mol above the barrier between the states. Thus, on our potential energy surface, the  $^2A_{1g}$  state does not exist as a separate species.

In the harmonic oscillator (HO) approximation the first excited vibrational level is three times as high above the potential energy minimum as the zero point level. While Figure 1 shows that the potential energy function of  $\text{C}_2\text{H}_6^+$  is certainly not

harmonic, and the levels may be somewhat lower than the simple HO model would predict, it still seems nearly certain that a single excitation of this low frequency C—C stretching vibration would place the vibrational energy above the barrier between the symmetric states, provided that the potential energy surface generated by our composite calculation is accurate.

Although the zero point level in the C—C stretch in the ground state is predicted to be about 0.5 kJ/mol below the top of the barrier, it is above the minimum of the  $^2A_{1g}$  state and intersects the potential energy surface where the barrier is only 0.03 Å wide. Since tunneling always occurs in a situation like this where it is feasible, the issue is not whether it will occur, but whether it will alter the observables significantly. The importance of tunneling can be expected to decrease with increasing separation of the states both in space and in energy. We think tunneling would not be highly significant in the ground state of  $C_2H_6^+$  on the following grounds: The mean square deviation from equilibrium of the lowest level of the HO is:  $\langle x^2 \rangle = h/8\pi^2\mu\nu$ , where  $h$  is Planck's constant,  $\mu$  is the reduced mass, and  $\nu$  is the HO frequency in hertz. This leads to a predicted root mean square (RMS) deviation of 0.0896 Å for the  $^2A_g$  state in the lowest vibrational level. The distance from the  $^2A_g$  minimum to the TS is 0.211 Å or 2.35 times this RMS deviation, while the separation between the minima (0.265 Å) is nearly three times this RMS deviation. The lowest level of the HO spends only 0.94% of its time at separations greater than 2.35 times the RMS deviation. The states are also separated in energy; the minimum of the  $^2A_{1g}$  state is only about 0.5 kJ/mol below the predicted ZPVE of the  $^2A_g$  state. Hence, the effect of tunneling on the zero point level is expected to be small. In light of the uncertainty regarding the C—C bond length in  $C_2H_6^+$ , we believe that this ion would be an interesting subject for a coulomb explosion experiment,<sup>10</sup> as that technique gives a snapshot of the vibrational amplitude probability distribution. Ions nearly this large have yielded interesting results by this method.

At the MP2/6-311 + G\*\* level the  $^2B_g$  state and the transition state (TS) have no single vibration for which C—C stretching forms a dominant component. Richartz et al. suggested that the  $^2B_g$  state was the most prominent one in the photoelectron spectrum (PES) of ethane.<sup>2</sup> Perhaps the lack of a normal mode devoted to C—C stretching is responsible for the absence of a clear vibrational progression in the PES, even though the ion and

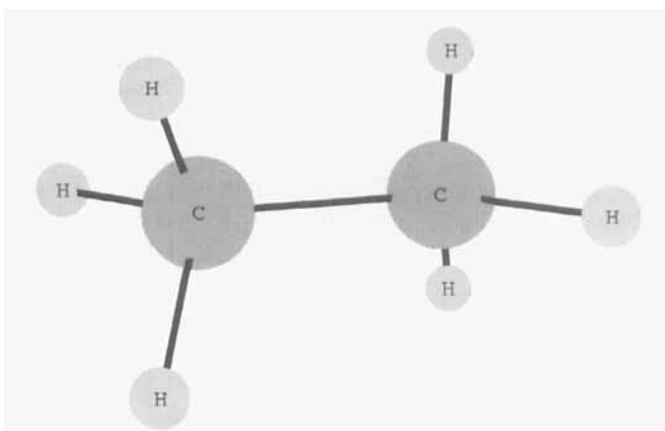


**FIGURE 3.** View of the  $^2B_g$  state of ionized ethane as optimized at the MP2/6-311 + G(2df,2p) level of theory.

neutral differ in C—C bond length by about 0.1 Å. In the transformation between symmetric states, the bridging hydrogens of the diborane-like form move more than the carbons. Hence, it is the motion of these atoms that dominate the imaginary vibration, at least at the MP2/6-311 + G\*\* TS. The data of Figure 1 yield a value of 2063i  $cm^{-1}$  for the imaginary frequency.

### Comparison of Theoretical Methods

Compared to the  $^2A_{1g}$  state, inclusion of  $f$  orbitals on carbon stabilizes both members of the  $E_g$  pair (after Jahn–Teller relaxation), which are not stable in UHF theory using smaller basis sets.<sup>4,6</sup> We sought to determine whether the inclusion of  $f$  orbitals would render the  $^2A_g$  and  $^2B_g$  stable by UHF methods. They do not. The structure of the  $^2A_g$  state as optimized by the MP2/6-311 + G(2df,2p) method was fed into an optimization using UHF theory in the same basis set. The result was convergence to the  $^2A_{1g}$  state. A similar UHF run with the  $^2B_g$  state converged to an optimized structure. However, Bouma et al.<sup>6</sup> found that a similar structure had two imaginary vibrational frequencies in UHF theory. The inclusion of  $f$  orbitals did not change this situation. Table IV shows that this state has only positive vibrational frequencies at the MP2 level. Polarization functions on carbon (but not on hydrogen) are necessary to achieve convergence to the ground state of  $C_2H_6^+$ . The  $^2A_g$  state forms a local minimum under MP2/6-31G\* theory with 18 positive vibrational frequencies. However, an attempt to optimize the structure using MP2/6-311 + G theory

(i.e., without polarization functions) converged to the  ${}^2A_{1g}$  state. When the nuclei are constrained to  $D_{3d}$  symmetry, the  ${}^2A_{1g}$  state is the only one found. Thus, a number of refinements (inclusion of electron correlation, use of polarization functions on carbon, and Jahn-Teller distortion) are necessary before calculations can find the  ${}^2A_g$  ground state of the ethane ion at all. Consideration of an odd number of excitations are necessary for the location of the  ${}^2A_g$  state as a minimum. CCD calculations failed to locate the state at all in the 6-311 + G(2df,p) basis set, converging on the  ${}^2A_{1g}$  state with RCC = 1.9275 Å. QCISD finds the diborane structure in a potential energy minimum, but place the long-bond state lower. The inclusion of triples in QCISD(T) finally brings QCI and MP2 methods into agreement that the  ${}^2A_g$  state is lowest.

### $D_{2h}$ Structure

Since the ground state of  $C_2H_6^+$  resembles the diborane structure, we wondered whether a  $C_2H_6^+$  having the full  $D_{2h}$  symmetry of diborane might be accessible. Accordingly, we constrained the ion to this symmetry and optimized the structure using the MP2/6-311 + G(2df,2p) method. This gave an energy of -79.192940 hartree, or 99.9 kJ/mol above the  ${}^2A_g$  state as computed at the same level of theory. The lowest energy fragmentation of ionized ethane is loss of  $H_2$ ,<sup>11</sup> which occurs 0.56 eV (54 kJ/mol) above the ionization potential of ethane.<sup>1,11</sup> The  $D_{2h}$  structure could serve as a TS for the simultaneous exchange of two hydrogen atoms between the carbons. Our results predict that this process should not occur readily below the fragmentation threshold. This is fully in accord with the finding of Lifschitz and Sternberg that  $CH_3CD_3^+$  showed a strong metastable peak for loss of HD, but that losses of  $H_2$  and  $D_2$  were absent.<sup>12</sup>

### Hyperfine Coupling Constants

We wished to compare the predictions of our calculations with the experimentally observed hyperfine coupling in the ethane cation radical. Most of the references we consulted give little explanation of how to do this.<sup>13</sup> Therefore, we explain our approach, which is not difficult, and has the added advantage of allowing the investigator to compensate for one defect of the calculation. The theory of

hyperfine couplings in ESR spectra holds that the coupling is proportional to the spin density at the nucleus.<sup>14</sup> From this belief we obtain eq. (1) which expresses this relation in terms of the spin density and coupling of the free hydrogen atom. All the constants in eq. (1) are known to high accuracy:

$$a^H(x) = [\rho^H(x)/\rho^H(H)]a^H(H) \quad (1)$$

where  $a^H(x)$  is the hydrogen coupling in the radical of interest,  $a^H(H)$  is the splitting in the free hydrogen atom, and  $\rho^H(x)$  and  $\rho^H(H)$  are the spin densities at the nuclei of the hydrogen atom in question and the free hydrogen atom, respectively. The spin density at each nucleus, as calculated by the method selected, is printed in the Fermi contact analysis section of the output from the Gaussian programs in units of electrons per cubic bohr. The spin density at the nucleus of the free hydrogen atom in these units is  $1/\pi$  from the hydrogen atom wave function. The term for hydrogen atom coupling at 9.5 GHz and including second-order corrections varies from 506.86 to 509.74 G,<sup>15</sup> depending on the size of  $a^H(x)$ . The precise figure can be calculated using the formulas of Wertz and Bolton,<sup>15</sup> but for couplings of less than 200 G the lower number is correct to 0.1% or better. It will be used here. The terms  $a^H(H)/\rho^H(H) = 506.86\pi$  G = 1592.3 G can be combined. Krogh-Jespersen and Roth have simplified this figure to 1600.<sup>16</sup> All of the theoretically predicted couplings for the  ${}^2A_g$  state of  $C_2H_6^+$ , whether obtained in this work using the 1592.3 constant of proportionality or published by Lunell and coworkers,<sup>5,9</sup> are below the experimental value. Part of the reason for this is probably that the Gaussian basis functions we and they employed are unable to adequately represent the wave functions at the hydrogen atom nuclei. The spin density calculated at the nucleus of the free hydrogen atom is 0.287444 in our largest basis set rather than the analytically correct  $1/\pi = 0.318310$ . Consequently, we insert the spin density for  $\rho^H(H)$  calculated in the same basis set<sup>17</sup> as  $\rho^H(x)$  into eq. (1).<sup>18</sup>

When this is done with the spin density of 0.086155 as calculated at the MP2/6-311 + G(2df,2p) minimum the result is 151.9 G, which is quite close to the experimental value<sup>3</sup> of 152.5 G. As noted previously, our highest level calculation predicts a substantially different structure for this ion than is obtained using MP2 methods. Principally the C—C bond is predicted to be longer by QCI methods than by MP2 methods. These longer

bond structures, whether arrived at by MP2 or QCI methods give hyperfine couplings that are smaller than the experimental one. For example, the run closest to the minimum in Figure 1 with  $\text{RC}-\text{C} = 1.65 \text{ \AA}$  gives a predicted spin density of 0.064819 using the MP2 density and 0.052878 using the SCF density. This leads to predicted hyperfine couplings of 114.3 and 93.2 G, respectively. The fact that these predicted couplings are substantially less than the experimental could be due to the inherent inaccuracy of the calculations, as one author concluded,<sup>19</sup> to the neglect of vibrational effects<sup>18</sup> (prohibitively time consuming in our largest basis set), or to the suggestion<sup>4</sup> that the matrix compresses the ion in the ESR experiment. Ion-induced dipole forces would be expected to cause such a compression, and Figure 1 shows that the energetic cost would be modest. The bond-lengthening effect of freezing the core (discussed above) probably also contributes to the gap between the observed and predicted couplings. The other four hydrogens in the  $^2A_g$  state are predicted to have couplings of  $-16.3 \text{ G}$  at the MP2/6-311 + G(2df,2p) minimum. These couplings are unresolved in the experiment.<sup>3</sup>

The  $^2B_g$  state is even more compact than the  $^2A_g$  state. However, it is also higher in energy at all levels of theory. Evidently, matrix effects are insufficient to render this state the most stable one. This state is predicted to have larger hyperfine couplings: four hydrogens of 177.4 G and two of  $-8.8 \text{ G}$  at the MP2/6-311 + G(2df,2p) minimum. The  $^2A_{1g}$  state is predicted to have six equivalent hydrogens of  $-9.1 \text{ G}$  splitting as calculated by the same method.

In summary, ionized ethane may have two or three "isomers."

## Facilities and Methods

All calculations were conducted using the GAUSSIAN 90 or GAUSSIAN 92<sup>20</sup> suites of programs as implemented on the Cray Y-MP computer at the University of Texas Center for High Performance Computing. In view of the small energy differences involved, all optimizations except for the  $D_{2h}$  structure were conducted with the command `opt = tight`. Tight optimization was achieved except as noted in this section. Tight optimization was nearly, but not quite, achieved in two runs not entered in the tables, but is discussed briefly in the text. These include the CCD opti-

mization of the long-bond form and the MP2 = frozen core optimization of the diborane form.

Several runs with the population analysis in natural orbitals suggested that the active space for the diborane form was not well defined. For example, in the geometry of our COMPOSITE optimum for the  $^2A_g$  state the orbital populations declined monotonically in occupancy with increasing energy of the orbital. The filled orbitals varied in occupancy from 2.00000 to 1.99505. The occupancy of the virtual orbitals ranged from 0.00495 to zero. Since these are all well outside the suggested occupancy limits of 0.02–1.98<sup>21</sup> for which CASSCF calculations are expected to be useful, we lost interest in calculations with a user-defined active space. However, one scientist strongly urged us to perform CASSCF calculations. These were attempted on the diborane form with orbitals 8 and 9; 7 and 9; 7, 8, and 9; and 8, 9, and 10 in the active spaces. In each case, the run terminated in the first optimization step with the conclusion: "You have chosen the wrong orbitals." Hoping that bond lengths closer to the TS between the  $^2A_g$  and  $^2A_{1g}$  states would give a more readily interpretable mixing of the orbitals, we tried `pop = no` runs with C—C bond lengths of 1.7 and 1.75 Å. The electron occupancies were similar to the results just described. The fact that triple excitations are necessary to find the experimentally observed state of the ethane ion lowest in energy means that the active space cannot be very small.

The MP2 calculations considered all electrons (MP2 = full) while the QCI calculations were with frozen core. The vibrational frequencies given in Table IV were calculated numerically from the MP2/6-311 + G(d,p) stationary points using MP2/6-311 + G(d,p) gradients. The frequencies are not scaled. The transition states were found by repeated tight optimization of the structure at fixed C—C bond distances. Optimization was considered complete when the residual force along this bond was less than 15 microhartrees per bohr. In the case of the MP2/6-311 + G(2df,2p) TS this criterion was never literally fulfilled. The results presented are the average of runs with the C—C bond fixed at 1.8522 Å (which had a residual force of  $-17$  microhartrees per bohr along the bond) and 1.8524 Å (with a residual force of  $+17$  microhartrees per bohr). These two runs had energies identical to eight significant figures. The optimized parameters of the composite method are the average of runs with C—C fixed at 1.65 and 1.66 Å for the  $^2A_g$  state. For the transition state and  $^2A_{1g}$  state the parameters are those for runs at 1.865 and 1.92



Å, respectively. Structures of lower symmetry were examined at lower levels of theory with the result that they collapsed to structures of symmetry  $C_{2h}$  (or  $D_{3d}$  in the case of the long-bond form). All structures discussed in this work were optimized with constraint to  $C_{2h}$  or  $D_{3d}$  symmetry. Spin densities are from the Fermi contact analysis using the MP2 density. At the MP2/6-311+G(2df,2p) minimum, the predicted splitting is not materially affected by using the SCF density (0.086160) instead of the MP2 density (0.086155). During the preparation of Figure 1 we made several runs calculating the QCISD(T) energy with the command density = current. The resulting output contained only results from the SCF density.

## Acknowledgments

We gratefully acknowledge the financial support (Grants H-609 to D. J. M. and BD1161 to C. S. G.) of the Robert A. Welch Foundation and the University of Texas Center for High Performance Computing for the use of its facilities. We also acknowledge helpful discussions with Santiago Olivella, who pointed out the necessity of using correlation methods in treating ionized alkanes, and with N. L. Bauld.

## References

1. S. G. Lias, J. E. Bartmess, J. F. Liebman, J. L. Holmes, R. D. Levin, and W. G. Mallard, *J. Phys. Chem. Ref. Data*, **17**, Suppl. 1 (1988).
2. A. Richartz, R. J. Buenker, P. J. Bruna, and S. D. Peyerimhoff, *Mol. Phys.*, **33**, 1345 (1977).
3. K. Toriyama, K. Nunome, and M. Iwasaki, *J. Chem. Phys.*, **77**, 5891 (1982).
4. D. J. Bellville and N. L. Bauld, *J. Am. Chem. Soc.*, **104**, 5700 (1982).
5. (a) S. Lunell and M.-B. Huang, *J. Chem. Soc. Chem. Commun.* 1031 (1989); (b) M.-B. Huang and S. Lunell, *Chem. Phys.*, **147**, 85 (1990).
6. W. J. Bouma, D. Poppinger, and L. Radom, *Israel J. Chem.*, **23**, 21 (1983).
7. S. M. Bråten, T. Helgaker, E. Uggerud, and T. Vilpius, *Org. Mass Spectrom.*, **28**, 1262 (1993).
8. L. A. Eriksson and S. Lunell, *J. Phys. Chem.*, **97**, 12215 (1993).
9. L. A. Eriksson, S. Lunell, and R. J. Boyd, *J. Am. Chem. Soc.*, **115**, 6896 (1993).
10. Z. Vager, R. Naaman, and E. P. Kanter, *Science*, **244**, 426 (1989).
11. W. A. Chupka and J. Berkowitz, *J. Chem. Phys.*, **47**, 2921 (1967).
12. C. Lifshitz and R. Sternberg, *Int. J. Mass Spectrom. Ion Phys.*, **2**, 303 (1969).
13. The method is fully explained in a way that is applicable to atoms other than hydrogen in the book W. Weltner Jr., *Magnetic Molecules and Atoms*, Dover, New York, 1972.
14. E. Fermi, *Z. Physik*, **60**, 320 (1930).
15. J. E. Wertz and J. R. Bolton, in *Electron Spin Resonance: Elementary Theory and Practical Applications*, McGraw-Hill, New York, 1972, p. 438 (Appendix C).
16. K. Krogh-Jespersen and H. D. Roth, *J. Am. Chem. Soc.*, **114**, 8388 (1992).
17. For the convenience of our readers we have calculated the spin density at the nucleus of the free hydrogen atom using the following commonly employed basis sets: N-21G 0.249785, N-31G 0.297902, 6-311G 0.287444, 6-311 + + G 0.287050. Polarization functions contribute neither to the hydrogen atom wave function nor to the Fermi contact term if present.
18. This approach has been used before, although it is not spelled out in quite such simple terms: D. Feller and E. R. Davidson, *J. Chem. Phys.*, **80**, 1006 (1984).
19. D. M. Chipman, I. Carmichael, and D. Feller, *J. Phys. Chem.*, **95**, 4702 (1991).
20. M. J. Frisch, M. Head-Gordon, G. W. Trucks, J. B. Foresman, H. B. Schlegel, K. Raghavachari, M. Robb, J. S. Binkley, C. Gonzales, D. J. Defrees, D. J. Fox, D. R. A. Whiteside, R. Seeger, J. J. P. Stewart, S. Topiol, and J. A. Pople, Gaussian 90, Gaussian Inc., Pittsburgh, PA, 1990.
21. P. Pulay, and T. P. Hamilton, *J. Chem. Phys.*, **88**, 4926 (1988).